Gel combustion synthesis and luminescence properties of nanoparticles of monoclinic SrAl$_2$O$_4$:Eu^{2+},Dy^{3+}

Ruixi Zhang, Gaoyi Han[*], Liwei Zhang, Binsheng Yang

Institute of Molecular Science, Chemical Biology and Molecular Engineering, Laboratory of the Ministry of Education, Shanxi University, Taiyuan 030006, PR China

ABSTRACT

Nanoparticles of strontium aluminate phosphors co-activated by Eu^{2+} and Dy^{3+} have been prepared by heating the precursors obtained from nitrate salt–ammonium acetic–urea–gel combustion process at temperature of 1150 °C in a weak reductive atmosphere of thermal carbon. Transmission electron microscope (TEM) images revealed that the hollow nanoparticles of SrAl$_2$O$_4$:Eu^{2+},Dy^{3+} were formed below 1150 °C, while the needle or rod-shaped particles were formed at 1200 °C. The XRD patterns indicated that the resulted SrAl$_2$O$_4$:Eu^{2+},Dy^{3+} nanoparticles contained distorted monoclinic lattice. The environment of rare earth ion in SrAl$_2$O$_4$ lattice was investigated by using Eu^{3+} as ion probe, and the results indicated that there were two kinds of sites occupied by Eu^{3+}, one was centro-symmetrical environment, while the other not. The luminescence and the afterglow properties of the hollow nanoparticles of SrAl$_2$O$_4$:Eu^{2+},Dy^{3+} were also investigated.

© 2008 Elsevier B.V. All rights reserved.

1. Introduction

Since the green- and blue-emitting long-lasting phosphorescence (LLP) phenomena of Eu^{2+}-doped alkaline earth aluminates MAl$_2$O$_4$:Eu^{2+} (M = Ca, Sr, Ba) were first found in 1996 by Matsuzawa et al. [1], further research revealed that the lifetime and intensity of the afterglow could be enhanced through co-doping with some other rare earth ions [2–4], and these oxide LLP materials have been developed to replace the conventional sulfide afterglow materials because of their good luminescent properties such as high initial luminescent intensity, long-lasting time, chemical stability, suitable emitting color and without radiation. These oxide phosphors exhibited a long period of luminescence after an initial rapid attenuation, and the lasting time of this new kind of phosphors was more than 10 times than that of the previous sulfide phosphors [5,6]. This long afterglow effect has been ascribed to the recombination between the trapped SrAl$_2$O$_4$:Eu,Dy electrons at europium(II) sites and the thermally released holes trapped at dysprosium(III) sites [7–11]. The detailed mechanism was not understood yet [9].

In most reports, the oxide LLP materials with large size were prepared by using solid-state reaction [1,12] and smaller particles must be obtained by grinding the larger phosphor particles, which can easily introduce additional defects and greatly reduce the luminescence efficiency [12]. With the development of technolo-

gies on materials, several kinds of chemical synthesis techniques such as co-precipitation [10], sol–gel [13,14], reverse microemulsion [15] and combustion methods [16–22] have been applied to prepare SrAl$_2$O$_4$ and its phosphors. Among these, combustion process was an interesting method to prepare the precursor powders. This synthesis technique used the heat energy released by the redox exothermic reaction between the metal nitrates and urea or other fuels at a relatively low-igniting temperature. The process was not only safe but also time and energy saving. Many materials have been prepared by using this process, for example, nano-SrAl$_2$O$_4$:Eu^{2+} was prepared by using metal nitrate–urea system [17] and nano-SrAl$_2$O$_4$:Eu^{2+},Dy^{3+} was prepared by using metal nitrate–glycine solution system [16]. Up to the present, many methods such as template method (hard templates or soft templates) [23–26], hydrothermal [27–29] and emulsion method [30] have been developed to prepare hollow particles of metal oxide. Furthermore, gel combustion process has been proved to be a convenient method for nanosized composite oxide [31]. In this paper, we reported the preparation of hollow SrAl$_2$O$_4$ phosphor nanoparticles doped with Eu^{2+} and Dy^{3+} by using gel combustion process. The solution of nitrate salt–ammonium acetic–urea mixture was heated at 85 °C until a gel formed, then the hollow nanoparticles precursors of SrAl$_2$O$_4$:Eu^{2+},Dy^{3+} were obtained by using the gel combustion process. After the resultant precursor powders were heated at 1150 °C in a weak reductive atmosphere of active carbon, the hollow particles of the phosphor with long afterglow were obtained. Moreover, the environment of the doping ion in matrix lattice was also investigated.

* Corresponding author. Tel.: +86 351 7010699; fax: +86 351 7016358.
E-mail address: han_gaoyis@sxu.edu.cn (G. Han).

2. Experimental

2.1. Materials

All the used reagents were of AR grade or higher quality and purchased from Beijing Chemical Reagent Company.

2.2. Synthesis of hollow nanoparticles of $SrAl_2O_4$:Eu,Dy phosphor

Dy_2O_3 (4 N) and Eu_2O_3 (4 N) were dissolved in small amount of HNO_3, then the solution was diluted to 0.10 M Dy^{3+} and Eu^{3+}, respectively. Then $SrCO_3$ (AR, 2.86 g) and $Al(NO_3)_3 \cdot 9H_2O$ (AR, 15.00 g) were added to the mixture solution of Dy^{3+} (4 ml) and Eu^{3+} (2 ml), respectively. After the $SrCO_3$ was dissolved completely, 10.0 ml distilled water, 20.0 g urea and 20.0 g ammonium acetic was added to the mixture. The mixture was heated at 85 °C for 15 h until the gel was formed. The obtained gel was then transferred into a muffle furnace maintained at 600 °C, and the gel boiled and underwent dehydration initially, then followed by decomposition with the evolution of large amounts of gases (oxides of carbon, nitrogen and ammonia), and finally, the foamy precursor was produced by the spontaneous combustion with enormous volume expansion. The whole process was over within less than 5 min.

The voluminous and foamy combustion ash was annealed at 800 °C at air atmosphere for 4 h to remove the residual carbon. The well-milled precursor powder was subsequently annealed at temperature range of 900–1200 °C for 2 h in an active carbon atmosphere to produce $SrAl_2O_4$:Eu^{2+},Dy^{3+} phosphor. In order to investigate the environment of the rare earth in the matrix lattice, the samples of $Sr_{0.97}Al_2O_4$:$Eu_{0.03}^{3+}$ were prepared in the similar process. For comparison, $Sr_{0.97}Al_2O_4$:$Eu_{0.01}^{2+}$,$Dy_{0.02}^{3+}$ phosphors were also synthesized at 1300 °C by using the usual solid-state reaction technique under a weak reductive atmosphere of active carbon, in which boric acid was added to the mixture as flux.

2.3. Characterization

The X-ray powder diffraction patterns were measured with a D8 Advance X-ray Diffractometer by using Cu Kα ($\lambda = 1.5406$ Å) radiation and the cell parameters were obtained by using Check Cell program. The morphological studies were carried out on a CSTM-9000 transmission electron microscope (TEM). Photoluminescence measurements were performed on a Hitachi F-2500 Spectrofluorometer at room temperature (for $SrAl_2O_4$:Eu,Dy phosphor and $Sr_{0.97}Al_2O_4$:$Eu_{0.03}^{3+}$ with 5 nm EX and EM slit). The decaying curves were also recorded by using the same instrument at room temperature (with 20 nm EM slit) after the samples had been excited sufficiently for about 5 min.

3. Results and discussion

The microstructure of the precursor powders and $SrAl_2O_4$:Eu^{2+},Dy^{3+} phosphor prepared at different temperatures is studied according to their TEM images shown in Fig. 1. The images illustrate that the hollow particles with irregular shapes are aggregated, and for some of them, parts of the walls are collapsed (Fig. 1A) for the precursor annealed at 800 °C, which is apparently different from traditional elliptic or circular $SrAl_2O_4$ crystal particles prepared by solution combustion process or other methods [17–19]. We may attribute the formation reason to the process of gel combustion although the formation of the hollow particles is not clear. With the increase of the temperature, the shape of the hollow particles become regular (Fig. 1B), and after being treated at 1150 °C for 2 h, the hollow elliptic particles have formed although the size distribution of hollow particles becomes wider (Fig. 1C). However, after the precursor has been annealed at 1200 °C for 2 h, the needle-like or rod-like crystal of $SrAl_2O_4$:Eu^{2+},Dy^{3+} is formed (Fig. 1D), this result is consistent with that of literature [10].

There are two phases in $SrAl_2O_4$, a high-temperature hexagonal phase and a low-temperature monoclinic phase. The transition temperature occurs at 650 °C. The XRD patterns of the $SrAl_2O_4$:Eu^{2+},Dy^{3+} prepared at various temperatures are shown in Fig. 2. Typical diffraction peaks of monoclinic phase with broad shape and low intensity together with diffraction peaks of a small
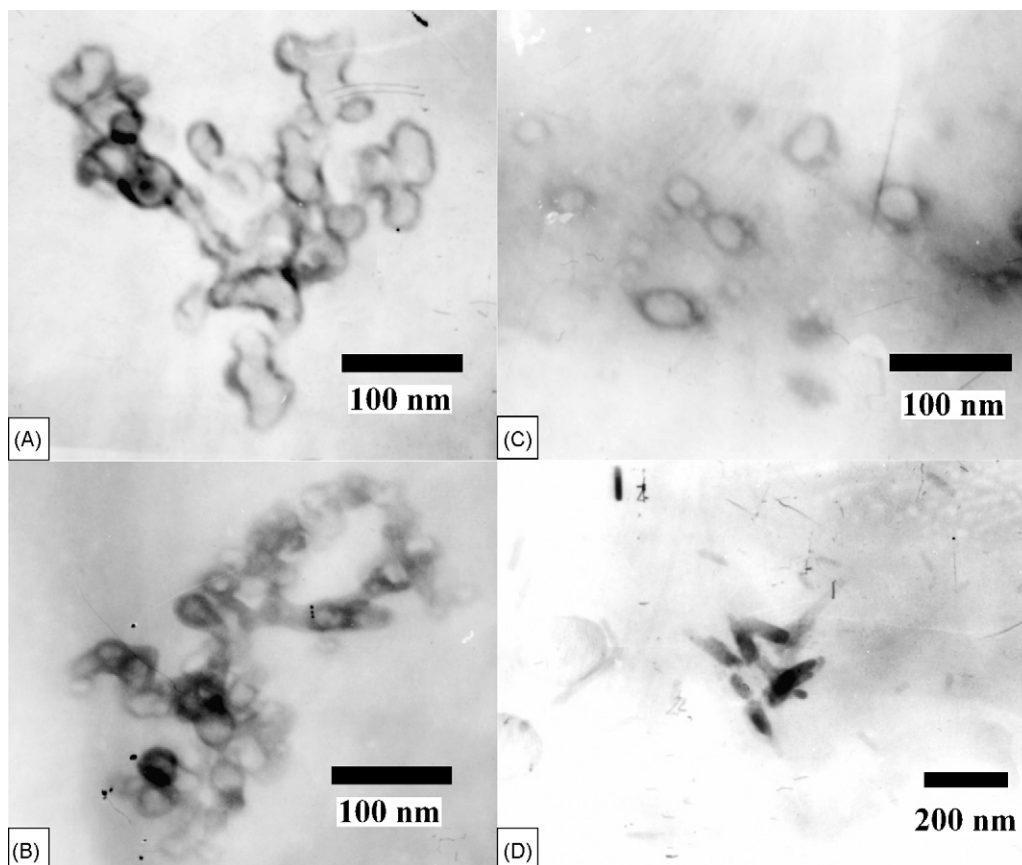

Fig. 1. The TEM images of the $SrAl_2O_4$:Eu^{2+},Dy^{3+} phosphors prepared by gel combustion precursors at different temperatures. (A) 800, (B) 900, (C) 1150 and (D) 1200 °C.
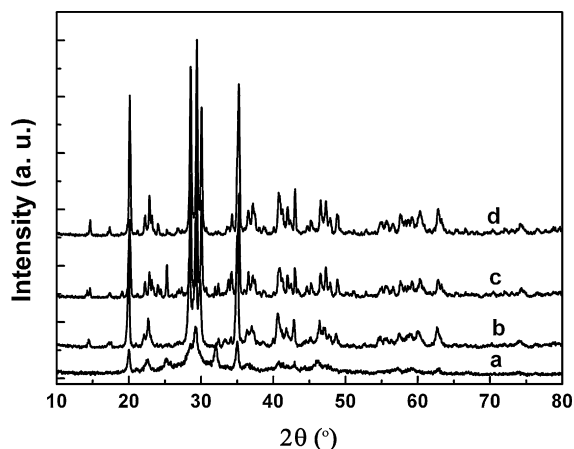
Fig. 2. The XRD patterns of $SrAl_2O_4:Eu^{2+},Dy^{3+}$ prepared by gel combustion precursors at various temperatures. (a) 800, (b) 1000, (c) 1200 and (d) 1150 °C.

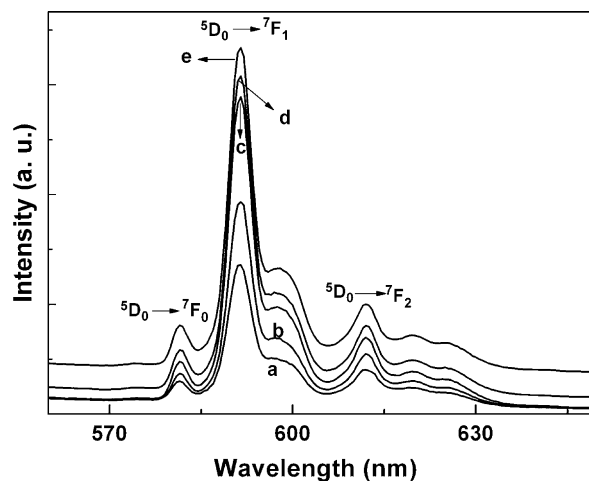**Fig. 3.** The fluorescence spectra of $Sr_{0.97}Al_2O_4:Eu_{0.03}^{3+}$ prepared by gel combustion precursors at different temperatures. (a) 900, (b) 1000, (c) 1100, (d) 1150 and (e) 1200 °C, $\lambda_{ex} = 234$ nm.

amount of other products (Fig. 2a) are observed for the samples sintered at 800 °C, which implies that the phase composition of the precursor powders is mainly low-temperature monoclinic phase although the crystal of $SrAl_2O_4$ is not developed perfectly. The little amount of doping rare earth (0.03 at.%) has almost no effect on the $SrAl_2O_4$ phase composition [10]. The results of our gel combustion are different from the earlier $SrAl_2O_4$ samples prepared by solution combustion process [17–19], in which diffraction peaks with high intensity assigned to monoclinic phase are dominant. The diffraction patterns of the samples sintered at higher temperatures show that all the peaks are due to the $SrAl_2O_4$ phase JCPDS (no. 34-379) and other crystal phases could not be detected. The intensity of the $SrAl_2O_4$ diffraction peaks increases (Fig. 2b–d) with the increase of thermal treatment temperature, which indicates that with the increase of annealed temperature, the crystal develops more perfectly. The highest diffraction intensity is observed for the phosphor prepared at 1150 °C (Fig. 2d). It is interesting that higher annealed temperature (1200 °C) leads to the decrease of diffraction intensity (Fig. 2c), which may be caused by the increasing defects during the morphology changes (from hollow particles to rod-shape). These results are different from prior results of conventional solid-state reactions, in which the pure $SrAl_2O_4:Eu,Dy$ monoclinic phase appears at 1300 °C [1]. In our system, although no flux is added, $SrAl_2O_4:Eu,Dy$ phase with high purity can be obtained at lower heat treatment temperature (900–1200 °C) by using gel combustion precursors, whereas it is impossible to happen for solid-state reaction method due to impurities of $M_3Al_2O_6$ formed at lower temperatures [1]. The reason may be attributed to the uniform components in gel, which is beneficial for the formation of the pure phase at relatively low temperature.

In addition, the refined crystallographic unit cell parameters are obtained and listed in Table 1. The values of the phosphors prepared by gel combustion precursors are roughly matched with $SrAl_2O_4$ standard values given in JCPDS (no. 34-379). From Table 1, we can

Table 1
Unit cell parameters for $Sr_{0.97}Al_2O_4:Eu^{2+},Dy^{3+}$ prepared by gel combustion precursors

Samples	α (Å)	b (Å)	c (Å)	β (°)	Cell volume (Å^3)
JCPDS no. 34-379	8.4470	8.8160	5.1630	93.42	383.797
Sample 800 °C	8.4171 (5)	8.8473 (5)	5.1413 (3)	93.17	382.278
Sample 1000 °C	8.4467 (4)	8.8575 (7)	5.1445 (5)	93.32	384.248
Sample 1150 °C	8.3984 (8)	8.7998 (4)	5.1355 (6)	93.39	378.869
Sample 1200 °C	8.3962 (6)	8.8019 (6)	5.1479 (5)	93.40	379.771

also find that the largest angle distortion ($\beta = 93.17$) is observed for samples prepared at 800 °C. With the increase of treated temperature, the values of β increase. A decrescent trend of unit cell parameters values can be observed compared with the standard values for all samples prepared by gel combustion precursor except that an increscent trend is observed for unit cell parameters b values when the precursors are treated at lower temperatures of 800 and 1000 °C.

Because the fluorescence of Eu^{3+} is very sensitive [32,33] to the coordinating surrounding, the samples of $Sr_{0.97}Al_2O_4:Eu_{0.03}^{3+}$ have also been prepared in the similar process to $SrAl_2O_4:Eu^{2+},Dy^{3+}$ in order to investigate the environment of rare earth ion. The emission spectra of $Sr_{0.97}Al_2O_4:Eu_{0.03}^{3+}$ prepared at different temperatures are shown in Fig. 3, from which, we can find that the emissions corresponding to $^5D_0 \rightarrow {}^7F_0$, $^5D_0 \rightarrow {}^7F_1$ and $^5D_0 \rightarrow {}^7F_2$ are located at 581, 591 and 612 nm, respectively. The emission of $^5D_0 \rightarrow {}^7F_1$ is more prominent, accompanied with the weak emission of $^5D_0 \rightarrow {}^7F_0$ and forbidden transition $^5D_0 \rightarrow {}^7F_2$. These results indicate that Eu^{3+} mainly lies in centro-symmetrical sites accompanied by a small amount of Eu^{3+} ions located at sites without inverse symmetry [31,32]. $SrAl_2O_4$ with b-tridymite structure belongs to the monoclinic $P2_1$ space group according to the literature [34,35]. In order to balance the charges, Sr^{2+} is located in the cavities of the framework being composed of AlO_4 tetrahedron. There are two kinds of low symmetric sites occupied by Sr^{2+}. The sizes of Eu^{2+} (1.20 Å), Eu^{3+} (1.01 Å), Dy^{3+} (0.97 Å) and Sr^{2+} (1.21 Å) are very similar, so that Eu^{2+} (1.20 Å), Eu^{3+} (1.01 Å), and Dy^{3+} (0.97 Å) ions can readily occupy the sites of Sr^{2+}. Therefore, it is expected that Eu^{3+} or $^{2+}$ should also lie in these two kinds of low symmetric sites. This result has been confirmed by EPR measurements in which reveal that there are two low symmetric sites occupied by Eu^{2+} in the stoichiometric $SrAl_2O_4$ [35–37]. Our results are consistent with the EPR measurements which also reveal Eu^{2+} occupies two kinds of sites. Furthermore, we can also find that one of the sites has centro-symmetrical surrounding, while the other has not symmetry of inversion.

The excitation and emission spectra at room temperature of $SrAl_2O_4:Eu^{2+},Dy^{3+}$ phosphor prepared by gel combustion and solid-state reaction methods are shown in Figs. 4 and 5. It is observed that the phosphors prepared by gel combustion precursors at different temperatures have similar excitation and emission spectra, in which three excitation bands are observed at 269, 320 and 350 nm corresponding to Eu^{2+} electron transition lying in the band gap
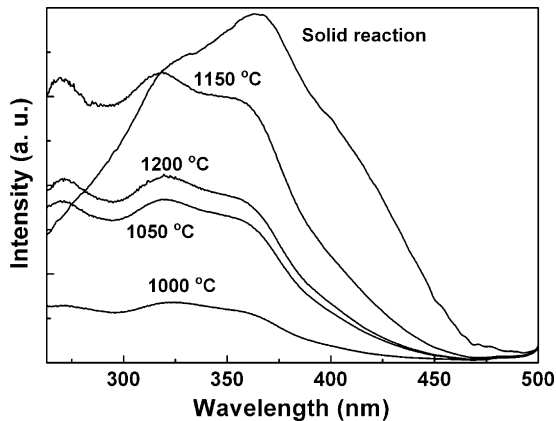
Fig. 4. Excitation spectra of the $Sr_{0.97}Al_2O_4:Eu_{0.01}{}^{2+},Dy_{0.02}{}^{3+}$ phosphors prepared by gel combustion precursors at different temperatures and by solid-state reaction, $\lambda_{em} = 511$ nm.

region of the host matrix, and the main excitation band is located at about 320 nm (Fig. 4). While the phosphor prepared by solid-state reaction method exhibits excitation bands at about 365 and 323 nm, and the main excitation band is located at about 365 nm (Fig. 4). Compared with the other studies for nanosized $SrAl_2O_4$ phosphors [14–16], the blue shift phenomenon is also found in our phosphors. The surface energy increases significantly when the grain size decreases to nanoscaled, which causes the change of the crystal field around the local environment of Eu^{2+} and the corresponding shift in the excitation spectra [15].

There is one emission band observed at 511 and 519 nm for phosphors prepared by gel combustion precursors and solid reaction, respectively (Fig. 5). Compared with the phosphors obtained from solid-state reaction method, the emission maximum band of phosphor prepared by gel combustion precursor shifts from 519 to 511 nm. The slight blue shift in the emission band may be attributed to the changes of the crystal field around Eu^{2+} arising from the nanosized particles. Since the excited $4f^6\,5d^1$ configuration of Eu^{2+} ion is extremely sensitive to the change in the lattice environment in contrast to the shielded $4f^7$ ground configurations, the 5d electron may couple strongly with the lattice. Therefore the mixed states of 4f and 5d will be influenced strongly by the crystal field. On the other hand, the particles with nanometer size make the surface energy increase significantly, which causes the change of the crystal field around the local environment of Eu^{2+}. These reasons may lead to
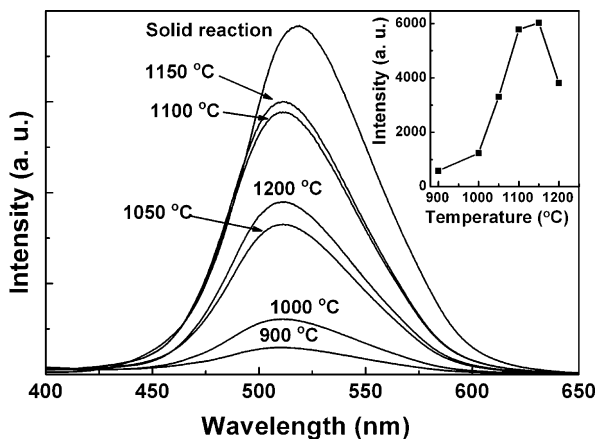

Fig. 5. Emission spectra of the $Sr_{0.97}Al_2O_4:Eu_{0.01}{}^{2+},Dy_{0.02}{}^{3+}$ phosphors prepared by gel combustion precursors at different temperatures and by solid-state reaction. $\lambda_{ex} = 350$ nm.
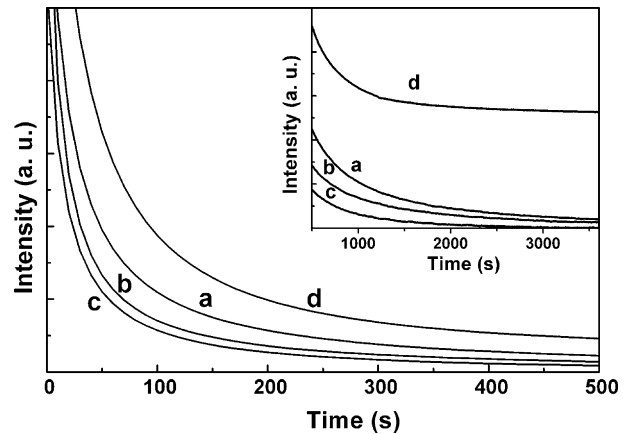

Fig. 6. The decaying curve of the $Sr_{0.97}Al_2O_4:Eu_{0.01}{}^{2+},Dy_{0.02}{}^{3+}$ phosphors after being excited for 5 min at room temperature (30 °C), phosphors prepare by gel combustion precursors at (a) 1150, (b) 1100, and (c) 1200 °C, respectively and (d) phosphor prepared by solid reaction method.

the blue shift of its emission peak [10,14]. Furthermore, we find that the fluorescence intensity of the phosphors prepared by gel combustion precursor is weaker than that by solid reaction method. This may be that a lot of defects are dispersed on the surface of phosphors because of the high surface area of the nanometer powders prepared by gel combustion precursors, which may result in the relatively less amount of luminescent center Eu^{2+} in the $SrAl_2O_4$ lattice available for direct radiation, therefore, it may result in the weaker fluorescence intensity.

When the gel combustion precursors are thermally treated at 900 °C in the weak reductive atmosphere for 2 h, weak afterglow phenomenon is observed after UV ray irradiation. The phosphor with the highest fluorescence intensity is obtained at treatment temperature of 1150 °C. Lower or higher annealed temperature will lead to a decrease in fluorescence intensity. These results are consistent with that of X-ray patterns. With the increase of the treatment temperature, the doping rare earth element could easily transfer into the lattice of the matrix, which results in the enhancement of the fluorescence intensity. Once the treatment temperature is higher than a threshold, can the microstructure of the phosphor change from hollow nanoparticles to needle or rod-like. We think that the microstructure change makes the fluorescence decrease because more defects have formed during the morphology change process.

Fig. 6 shows the decaying curve of $SrAl_2O_4:Eu^{2+},Dy^{3+}$ phosphor powders. The results indicate that the decaying processes of both the two kinds of phosphors contain a rapid-decaying process and a slow-decaying one. The initial intensity of phosphor powders prepared by the gel combustion method is lower than that prepared by the solid-state reaction method. Moreover, the phosphors prepared by gel combustion decay more rapidly (Fig. 6a–c) than that prepared by the solid-state reaction method (Fig. 6d). We can also find that the samples prepared by gel combustion precursors at 1150 °C exhibit better afterglow property than that at 1100 and 1200 °C. And the afterglow property of samples prepared at 1200 °C is the lowest among these three samples due to the microstructure change from hollow particles to needle or rod-shaped particles. The reason is possibly that the phosphor particles prepared by gel combustion precursors are so small that the phosphor crystallizes easily, and Eu and Dy ions could be easily transferred into the $SrAl_2O_4$ crystal lattice during heat treatment process. The amount of defects may be decreased in the inner phosphor and the trap level becomes shallower simultaneously than that of phosphor obtained from solid-state reaction method, the relative intensity of afterglow is

lowered and the decaying process of afterglow is faster. In addition, a lot of defects are dispersed on the surface of the nanometer particles because of the high surface area, which may result in the weaker initial intensity of the phosphors prepared by gel combustion precursor because of less amount of luminescent center Eu^{2+} in the $SrAl_2O_4$ lattice available for direct radiation.

4. Conclusion

The hollow nanoparticles of $SrAl_2O_4$:Eu,Dy phosphor have been synthesized by gel combustion procedure, followed by heating the resultant combustion precursor powder at 900–1150 °C in a weak reductive atmosphere of active carbon. This gel combustion process may be used to prepare other metal oxides. Analytical results show that the nanometer phosphors have pure monoclinic $SrAl_2O_4$:Eu,Dy phase. There are two kinds of sites occupied by rare earth ion, one is centro-symmetrical environment while the other not. Compared with the solid-state reaction method, the blue shift of main peaks of excitation and emission of the nanometer phosphors occurs.

Acknowledgement

References

[1] T. Matsuzawa, Y. Aoki, N. Takeuchi, Y. Murayama, J. Electrochem. Soc. 143 (1996) 2670.
[2] I.C. Chen, T.M. Chen, J. Mater. Res. 16 (2001) 644.
[3] Z.G. Wei, L.D. Sun, C.S. Liao, J.L. Yin, X.C. Jiang, C.H. Yan, S. Lu, J. Phys. Chem. B 106 (2002) 10610.
[4] Z.W. Wei, X. Mei, Z.W. Ping, Y. Min, Q.Z. Ming, X.S. Da, C. Garapon, Chem. Phys. Lett. 376 (2003) 318.
[5] E. Nakazawa, T. Mochida, J. Lumin. 72–74 (1997) 236.
[6] Y.L. Liu, B.F. Lei, C.S. Shi, Chem. Mater. 17 (2005) 2108.
[7] M.D. Segall, P.L.D. Lindan, M.J. Probert, C.J. Pickard, P.J. Hasnip, S.J. Clark, M.C. Payne, J. Phys. Condens. Mater. 14 (2004) 2717.
[8] J.P. Perdew, S. Burke, M. Ernzerhof, Phys. Rev. Lett. 77 (1996) 3865.
[9] T. Aitasalo, J. Holsa, H. Jungner, M. Lastusaari, J. Niittykoski, J. Alloys Comp. 341 (2002) 76.
[10] Y.H. Lin, Z.T. Zhang, F. Zhang, Z.L. Tang, Q.M. Chen, Mater. Chem. Phys. 65 (2000) 103.
[11] W.Y. Jia, H.B. Yuan, L.Z. Lu, H.M. Liu, W.M. Yen, J. Lumin. 76–77 (1998) 424.
[12] R.P. Rao, J. Electrochem. Soc. 143 (1994) 189.
[13] L.K. Kurihara, S.L. Suib, Chem. Mater. 5 (1993) 609.
[14] T.Y. Peng, H.J. Liu, H.P. Yang, C.H. Yan, Mater. Chem. Phys. 85 (2004) 68.
[15] C.H. Lu, S.Y. Chen, C.H. Hsu, Mater. Sci. Eng. B 140 (2007) 218.
[16] T.Y. Peng, H.P. Yang, X.L. Pu, B. Hu, Z.C. Jiang, C.H. Yan, Mater. Lett. 58 (2004) 352.
[17] Z.L. Fu, S.H. Zhou, Y.N. Yu, S.Y. Zhang, Chem. Phys. Lett. 395 (2004) 285.
[18] J.J. Kingsley, K. Suersh, K.C. Patil, J. Mater. Sci. 25 (1990) 1305.
[19] Z.L. Fu, S.H. Zhou, S.Y. Zhang, J. Phys. Chem. B 109 (2005) 14396.
[20] Y.P. Fu, J. Alloys Comp. 402 (2005) 233.
[21] J. Dhanaraj, R. Jagannathan, T.R.N. Kutty, C.H. Lu, J. Phys. Chem. B 105 (2001) 11098.
[22] S.K. Shi, J.Y. Wang, J. Alloys Comp. 327 (2001) 82.
[23] Y.D. Xia, R. Mokaya, J. Mater. Chem. 15 (2005) 3126.
[24] Z.B. Lei, J.M. Li, Y.X. Ke, Y.G. Zhang, H.C. Zhang, F.Q. Li, J.Y. Xing, J. Mater. Chem. 11 (2001) 2930.
[25] E.S. Kang, M. Takahashi, Y. Tokuda, T. Yoko, Langmuir 22 (2006) 5220.
[26] S.Y. Gao, H.J. Zhang, X.M. Wang, R.P. Deng, D.H. Sun, G.L. Zheng, J. Phys. Chem. B 110 (2006) 15847.
[27] X.M. Sun, J.F. Liu, Y.D. Li, Chem. Mater. 18 (2006) 3486.
[28] H.L. Zhu, K.H. Yao, H. Zhang, D.R. Yang, J. Phys. Chem. B 109 (2005) 20676.
[29] M.M. Titirici, M. Antonietti, A. Thomas, Chem. Mater. 18 (2006) 3808.
[30] Y.X. Pang, X.J. Bao, J. Mater. Chem. 12 (2002) 3699.
[31] C. Cannas, A. Musinu, D. Peddis, G. Piccaluga, Chem. Mater. 18 (2006) 3835.
[32] S.K. Ruan, J.G. Zhou, A.M. Zhong, J.F. Duan, X.B. Yang, M.Z. Su, J. Alloys Comp. 275–277 (1998) 72.
[33] Y.H. Zhou, J. Lin, S.B. Wang, H.J. Zhang, Opt. Mater. 20 (2002) 13.
[34] F. Clabau, X. Rocquefelte, S. Jobic, P. Deniard, M.H. Whangbo, A. Garcia, T. Le Mercier, Chem. Mater. 17 (2005) 3904.
[35] T. Nakamura, K. Kaiya, N. Takahashi, T. Matsuzawa, M. Ohta, C.C. Rowlands, G.M. Smith, P.C. Riedi, Phys. Chem. Chem. Phys. 3 (2001) 1721.
[36] T. Nakamura, K. Kaiya, N. Takahashi, T. Matsuzawa, C.C. Rowlands, V. Beltran-Lopez, G.M. Smithf, P.C. Riedi, J. Mater. Chem. 10 (2000) 2566.
[37] K. Kaiya, N. Takahashi, T. Nakamura, T. Matsuzawa, G.M. Smith, P.C. Riedi, J. Lumin. 87–89 (2000) 1073.